La radiologia medica (2021) 126:380–387
https://doi.org/10.1007/s11547-020-01271-2

CHEST RADIOLOGY

Radiation dose reduction considerations and imaging patterns of ground glass opacities in coronavirus: risk of over exposure in computed tomography

Mohammad Ahmmad Rawashdeh[1] · **Charbel Saade**[2]

Received: 28 April 2020 / Accepted: 23 August 2020 / Published online: 8 September 2020
© Italian Society of Medical Radiology 2020

Abstract
This article aims to summarize the available data on the severe acute respiratory syndrome coronavirus 2 (SAR-CoV-2) imaging patterns as well as reducing radiation dose exposure in chest computed tomography (CT) protocols. First, the general aspects of radiation dose in CT and radiation risk are discussed, followed by the effect of changing parameters on image quality. This article attempts to highlight some of the common chest CT signs that radiologists and emergency physicians are likely to encounter. With the increasing trend of using chest CT scans as an imaging tool to diagnose and monitor SAR-CoV-2, we emphasize that pattern recognition is the key, and this pictorial essay should serve as a guide to help establish correct diagnosis coupled with correct scanner parameters to reduce radiation dose without affecting imaging quality in this tragic pandemic the world is facing.

Keywords COVID-19 · Multidetector computed tomography · Infections · Virology

Introduction

The rapid rise of severe acute respiratory syndrome coronavirus 2 (SARS-CoV-2; previously known as 2019 novel coronavirus or 2019-nCoV) disease (COVID-19) has become a global emergency that has sent shockwaves in medicine to each corner of the globe [1]. The coronavirus infection took place in Wuhan, Hubei Province, China. In humans, coronaviruses are a series of viruses that cause the symptoms of upper respiratory infections which can become severe. The current status of mortality rates between China and Italy are similar with fatalities in mostly the elderly with known comorbidities [2]. Severe acute respiratory syndrome (SARS) and Middle East respiratory syndrome (MERS) have mortality rates of 10% and 37%, in each of their respective continents [1, 3, 4]. This global emergency has resulted in increased utilization of chest imaging in the confirmation and progress of disease throughout their treatment.

Over the last century, chest radiography was the first line of imaging in respiratory related pandemics that occurred such as Malaria, Influenza, Tuberculosis, SARS and HIV/AIDS [5]. However, the explosion of computed tomography (CT) technology and the effect of lower doses in chest CT around the world have been heavily employed to monitor SARS-CoV-2 [6–10]. Standard chest CT doses can range from 3 to 4.8 mSv and low/ultra-low dose chest CT 0.13–1.5 mSv [11, 12]. A recent study demonstrated that no effect of low-dose CT on human DNA was detected with chest CT scans below 1.5 mSv, and increasing beyond this dose increases double-strand breaks in DNA and chromosome aberrations [13]. As such, depending on the severity of disease in SARS-Covid-2, the mean time between the first CT and the subsequent CT range from mild, common, severe and critical is from 5.8 ± 1.2, 4.9 ± 1.4, 4.5 ± 1.0 and 3.7 ± 1.1 days, respectively [14]. Therefore, in the current global pandemic there have been patients undergoing routine chest CT examinations up to 14 CT scans in the monitoring of disease [15], which can potentially place the patient at risk with a combined radiation dose delivered

✉ Charbel Saade
cs39@aub.edu.lb

Mohammad Ahmmad Rawashdeh
marawashdeh@just.edu.jo

[1] Department of Allied Medical Sciences, Jordan University of Science and Technology, P.O.Box 3030, Irbid 22110, Jordan

[2] Diagnostic Radiology Department, American University of Beirut Medical Center, P.O.Box 11-0236, Riad El-Solh, Beirut 1107 2020, Lebanon

within 20 days from 21 to 67 mSv which the latter has up to 3.5 times the allowable dose as per the recommendations set by the International Commission on Radiological Protection (ICRP) Report 103 [16].

As of April 27, 2020, a total of 3,017,806 cases and 209,661 deaths had been reported in more than 100 countries [17]. With this ever-expanding number of SARS-CoV-2 cases, the radiological society bodies [18, 19] were first to release statements that the first line of imaging should be a chest radiograph and not a chest CT. Prior to conducting this retrospective review, the institutional review board approval was waived. The aim of this review is to highlight the scanning techniques that reduce radiation dose without affecting imaging quality in low-dose lung CT in the diagnosis of ground glass opacities (GGO).

Anatomical considerations

The anatomy of the secondary pulmonary lobule is key to understanding of GGO. The identification of the patterns of infiltration and distribution is a key to the establishment of a correct list of differential diagnoses, and sometimes to the diagnosis itself [20]. CT provides submillimeter spatial and contrast resolution into lung parenchymal anatomy and architecture. The following anatomic structures and architectural components need to be considered:

Secondary pulmonary lobule

The secondary pulmonary lobule (SPL) is the smallest anatomical unit of the lung parenchyma that can be visualized on CT examinations (Fig. 1). SPL is a fundamental unit of lung structure, and an understanding of lobular anatomy is essential to the interpretation of thin-section CT of the lung [21]. Whereas in normal lung parenchyma, these polyhedral structures (size range: 1–2.5 cm diameter) [21] are only visualized in the anterior and lateral aspects of lung parenchyma, these become clearer when interstitial lung disease is present [20]. The SPL is surrounded by connective tissue septa. A central bronchovascular bundle, consisting of the pulmonary bronchiole and artery, perforates the center of the SPL, where the bronchiole divides into three to five terminal bronchioles [20]. At the origin of the terminal bronchioles is termed the "centrilobular" region.

The acinus is located within the SPL. It is a portion of lung distal to a terminal bronchiole (the last purely conducting airway) and is supplied by a first-order respiratory bronchiole or bronchioles [22, 23]. Acini size ranges from 6 to 10 mm in diameter [24]. Therefore, on thin-section CT images, the secondary pulmonary lobule can be divided into three components: the interlobular septa; the centrilobular region; and the lobular parenchyma.

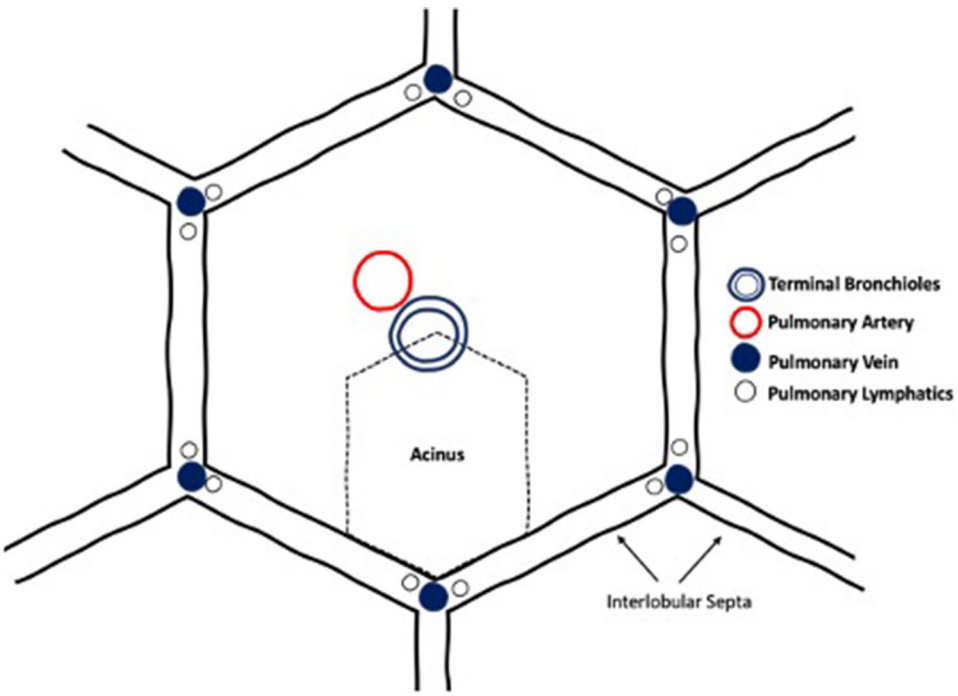

Fig. 1 Secondary pulmonary lobule (*P*ulmonary arteries and bronchioles with a diameter of approximately 1 mm; interlobular septa with a thickness of approximately 0.1 mm; pulmonary vein and lymphatic branch with diameters of 0.5 mm each; and acinus—never visible on CT scans)

Interlobular septa

Secondary pulmonary lobule (SPL) is surrounded by the connective-tissue interlobular septa (ILS) that extend from the pleural surface of the lung inward [21]. The ILS consists of connective tissue, house pulmonary veins, and lymphatics and belongs to the peripheral interstitial fiber system. Interestingly, the pulmonary veins traverse within ILS and not parallel to the segmental or sub-segmental pulmonary artery branches and bronchi [22]. ILS are well matured in the lung periphery and most abundant in the apices of the lungs. They are concentrated near the anterior, lower, mediastinal, and diaphragmatic surfaces of the lung. Interestingly, the key structures for identifying SARS-CoV-2 have demonstrated thickening and increased visualization of these ILS at these anatomical locations [1, 4, 25].

Centrilobular region

The centrilobular region consists of the pulmonary artery and bronchioles that supply the SPL. Due to the complexity of the branches of the terminal bronchioles, branching generation is almost difficult to define and trace which branch of the pulmonary arteries and veins are aligned with the bronchioles that supply the SPL. Anatomically, lobular bronchioles are rarely seen under CT in normal individuals since their lumen measures approximately 1 mm in diameter, and their wall 0.15 mm, respectively [23]. However, the centrilobular region is well visualized through thickened walls, peribronchiolar inflammation, and/or intrabronchiolar fluid and mucus accumulations. Radiologically, they are best seen in the lung periphery which is more evident in patients with known SARS-CoV-2 [6, 10, 26].

Lobular parenchyma

Lobular parenchymal consists of the structures between outer septa and the centrilobular structures: which include the acini and intralobular septa which contain the pulmonary capillary bed [21]. These structures like others in the SPL are not visible by CT in healthy patients; however, in patients with known SARS-CoV-2, increased attenuation is seen [27].

Imaging characteristics

Ground glass opacity and SARS-CoV-2

Detection and management of GGO is an important imaging characteristic in SARS-CoV-2 screening, because persistent GGO are often a sign of poor progression in disease treatment [9, 14]. GGO is an area of hazy increased lung density with preservation of underlying bronchovascular margins that when obscured, they then form to become consolidation. However, imaging pitfalls exist by the following: 1: normally seen with exhalation, 2: volume averaging with thick collimation greater than 5 mm, 3: window settings too narrow, 4: independent from lung atelectasis, and finally 5: motion artifact due to respiration [28]. However, when reviewing the radiology-pathology correlation firstly, there is partial airspace filling by edema, hemorrhage and infection and secondly, interstitial thickening by inflammation edema or fibrosis. Therefore, the presence of consolidation can suggest that radiological characteristics of GGO demonstrate alveolar filling with the presence of reticular opacities or traction bronchiectasis suggests and interstitial thickening (and with traction bronchiectasis, fibrosis).

With the outbreak, a wide array literature has flooded the research environment with SARS-CoV-2 imaging patterns. The earliest description of GGO occurred with bilateral lung involvement on initial chest CT and then changed with time to become a consolidative pattern [29] (Fig. 2). This demonstrated a series of abnormal findings in 86% of patients, with a majority involving the lung parenchyma bilaterally [6] (Fig. 3).

Degree of confidence

When the radiologist is reporting he/she shall choose the degree of confidence based on the CT findings. The most discriminating features for SARS-CoV-2 pneumonia included a peripheral distribution (80% vs. 57%, $p < 0.001$), ground-glass opacity (91% vs. 68%, $p < 0.001$) and vascular thickening (58% vs. 22%, $p < 0.001$) [30]. This was further validated between Chinese and US radiologists sensitivities (CHN:72–95%; USA: 73–93%) and specificities (CHN:24–94%; USA:93–100%) [30] with mixed results. Therefore, there are four degrees of confidence which are as follows:

1. *High confidence* will involve obvious peripheral, bilateral (multilobular), GGO with or without consolidation or intermixed septal thickening and multifocal GGO of rounded morphology with or without consolidation.
2. *Intermediate confidence* will involve GGO with or without consolidation that is not with a clear distribution and non-rounded and is also unilateral with or without consolidation.
3. *Low confidence* will demonstrate low patterns of consolidation without GGO and is very few in small GGO with non-rounded and non-peripheral distribution.
4. *Alternative diagnosis* the CT features demonstrate discrete nodules such as centrilobular, tree in bud, rounded small nodules, cavitation, perihilar GGO (with no

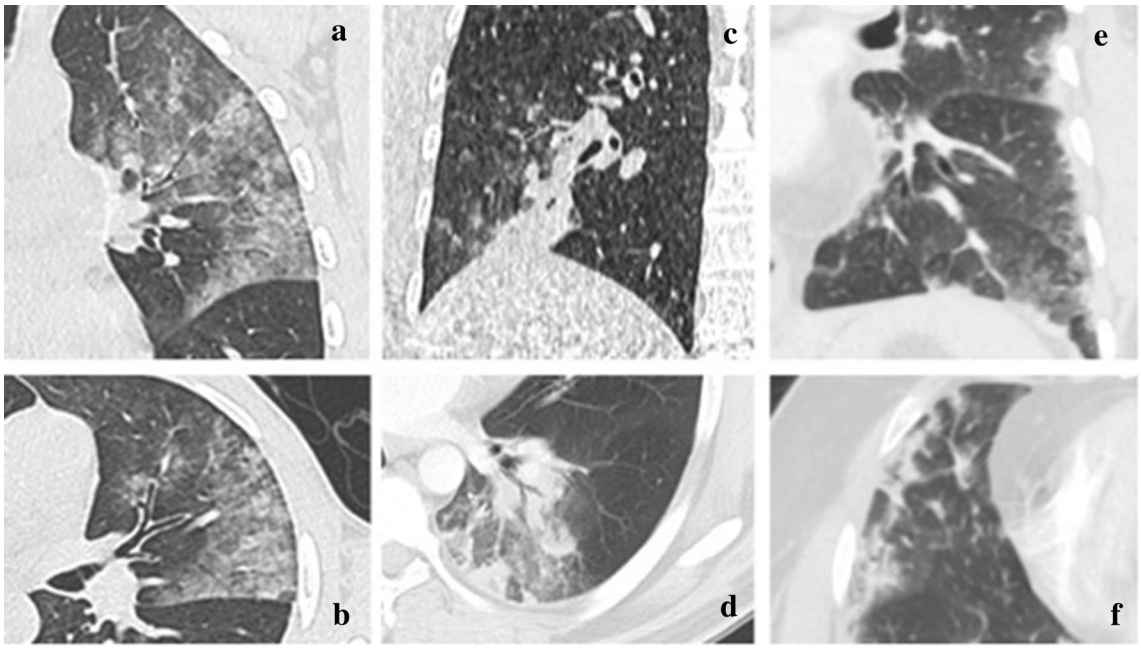

Fig. 2 Top row demonstrates coronal reformats, and the bottom row axial sections: **a**, **b** ground glass opacity, **c**, **d** consolidation w air bronchogram and ground glass shadows and **e**, **f** multifocal interstitial and alveolar shadows

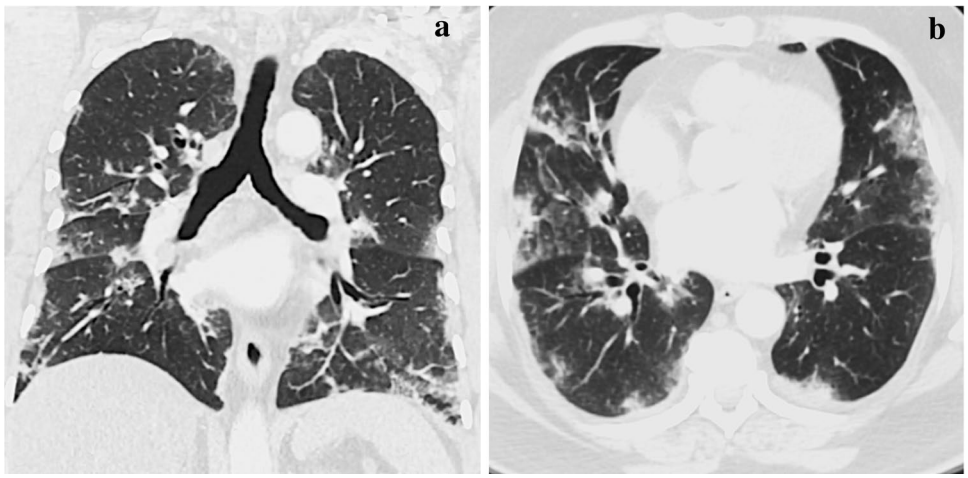

Fig. 3 63-year-old male presented with fever, dry cough, and chest pain for 4 days. He had a positive PCR and confirmed peripheral and central GGO bilaterally which was confirmed it was SARS-CoV-2

peripheral GGO), smooth septal thickening with pleural effusions and fibrosis.

Principles of CT radiation dose reduction

The visualization of structures during low-dose CT (LDCT), one must consider the variable exposure that can be used in CT imaging and the fact that CT as an imaging modality is capable of yielding high radiation dose to the patient [31]. The mantra of ALARA (As Low as Reasonably Achievable) with CT scanning dictates that lung screening for SARS-CoV-2 may only be feasible if low-dose scans are employed. In this section, we will discuss the importance of LDCT in the imaging of GGO and consolidation as part of the imaging considerations in detecting disease.

There are a wide array of factors that can influence the radiation dose either directly or indirectly which can result in safe dose reduction without affecting image quality. First and foremost, it should be stated that radiation dose to the patient can be significantly reduced by carefully following proper techniques such as 1: correct patient centering by placing the chest in the center of the field of view [32], 2: reduce scan unnecessary scan length without affecting image quality [33], 3: shielding radiosensitive organs such as the mammary gland employing bismuth shields [34, 35],

4: organ-based tube current modulation [36] and 5: the radiologist screening unnecessary requests for CT scans [37].

The scanning parameters employed in the detection of GGO and consolidation involve: 1: modification of tube current is the simplest method of radiation dose reduction and has been a mainstay of radiation dose reduction methods [32], 2: employing 100 kVp protocol can reduce radiation dose by 44% while maintaining low-contrast detectability compared with a 120 kVp protocol [38], 3: helical pitch (< 1.3 mm) and collimation (40–80 mm) has no effect on image quality and in-plane resolution [39], 4: correct patient centering [40] in order to have optimal performance of the automatic exposure control with tailored according to patient weight, patients are potentially exposed to a 17–43% higher radiation dose from a chest CT [41] and 5: employing iterative reconstruction with low kVp is that of those when scanning with 120 kVp with the sensitivity to detect ground-glass opacities, ground-glass nodules and interstitial opacities decreased significantly, from 89% to 77%, 86% to 68% and 91% to 71%, respectively (all p values < 0.00001) [42] (Table 1).

The detectability of lesions in CT chest scans (standard and low dose) can be variable between readers. Firstly, the performance of expert readers in lesion detection, including studies carried out on anthropomorphic phantoms [31, 43] and on lung trials with human participants [44, 45], will be discussed. Secondly, highlighting the scanning parameters of LDCT, the effect of a change in mA and image quality, and how those changes affect reader's performance.

The reduction of radiation doses is remarkable between standard-dose CT and 50%-reduced-dose CT were 15.6–21.4 mSv and 7.8–10.7 mSv, respectively [46]. Zhu et al. (2008) also found that there was no significant compromise to image quality between CT chest scans that were obtained at 25 mAs and 115 mAs [47]. On the other spectrum, Li et al. (2002) report that lung opacities were missed on LDCT screening due overlapping structures, small faint nodules and opacities in the anatomical background. Furthermore, in this study, out of the 39 CT scans, 32 lung cancers were missed: 23 scans owing to detection errors and 16 scans owing to interpretation errors [48]. To reconcile findings between Zhu et al. (2008) and Li et al. (2002), Kubo et al. (2008) have reported in a review of five studies that a low–dose range of 20–50 mAs was sufficient for the detection of pulmonary nodules which can be those of GGO also [40, 47, 48].

When considering the effect of mA upon image quality, there is some evidence to show little significant statistical difference in the determination of image quality between CT chest scans that were obtained at 25 mAs and 115 mAs [47]. In a study by Prasad et al. (2002), it was reported that a 50%-reduction in radiation dose for chest CT patients still allowed for adequate visualization of the

Table 1 Summation of the factors that affect dose and image quality in CT scanning

Parameters affecting dose reduction	Effect on image quality	Remedies
Tube current (mAs)	Image noise will increase as radiation dose decreases	Weight-based protocols Noise Index threshold
Tube voltage (kVp)	A lower kVp setting can result in a substantial decrease in radiation dose and increase in image noise and low contrast resolution structures	100 kVp
Helical pitch	Increasing the pitch shortens the scanning time, therefore, decreasing dose, which in turn increases noise	Collimation 40–80 mm section thickness < 1.5 mm [20] 1 mm/rot > Pitch < 1.3 mm/rot
Scan range	The dose increases linearly, as scan length is increased	From apices to costophrenic recess
Automatic exposure control	Significant dose reductions by exposure adjustment to the overall size of a patient's body, without significant change in image quality	Center the patient in the isocenter to prevent mA modulation over- or under-compensation of the airgap from the tube to the detector
Temporal resolution	Respiratory artifacts will reduce significantly due to the patients' respiratory condition	Temporal resolution < 0.5 s
Iterative reconstruction	Can alter the texture pattern which is dependent on tube potential and current	Employ a gradual increase between hybrid and model-based iterative reconstruction and always compare it to filtered back projection as the gold standard

central and peripheral lung parenchyma. Another similar study found that the reduction of radiation dose between standard-dose CT and 50%-reduced-dose CT that could be achieved with acceptable image quality was up to 50%, from 15.6–21.4 mSv down to 7.8–10.7 mSv, respectively [46]. Gunnar (2013) has also reported that there was no impact upon the mean sensitivity of readers when viewing scans of lower image quality (those taken at 150 mAs compared with 40 mAs) [49]. Finally, image noise is key to determine the tube current needed to obtain the desired image quality at the prescribed noise index. Higher image noise implies the need for lower radiation dose. Lower image noise, on the other hand, needs increased radiation dose to achieve lower image noise or higher image quality [50]. This can be adjusted based on optimal patient centering in the center of the gantry and the mA modulation in both *x*, *y* and *z* will adjust to provide both minimum and maximum mA relative to the patient habitus.

Gordic et al. (2014) reported that dose levels achieved using LDCT (0.06 mSv) [31] were comparable to conventional CXR study (0.02 mSv for a PA CXR to 0.1 mSv for the lateral CXR) making LDCT an ethical choice on the radiation dose front [51]. Although Gordic et al. (2014) used an anthropomorphic phantom of an average size adult in their study, the results suggest that dose delivered to a human in the course of detection for pulmonary lesions/opacities can be reduced to 0.06 mSv when using a single-energy scanner at 100 kVp.

Zhu et al. (2004) on the other hand found that quality of a CT chest deteriorates when the mA is reduced, causing the noise levels to increase, and thereby affecting image quality. Various mAs (25, 40 and 115) levels were analyzed for image quality in chest CT and found that 25mAs or greater was a sufficient exposure parameter for the detection of pulmonary nodules. Exposure factors below 25 mAs were considered unsatisfactory, when examining nodules on lung window settings, due to the compromise of image quality and the change in noise levels [47].

GGO detection using LDCT

The fundamentals of clinical scanning should be to assist in the diagnosis (or exclusion) of disease, and therefore if the same clinical questions can be answered with a LDCT scan as a standard-dose CT scan, then the imperative to reduce the dose is more important than the overall image quality of the scan per say (24). In the early millennia, Kubo et al. (2008) attempted to study the visual search patterns when viewing CT images and possible disturbances when reducing image quality. Kubo et al. (2008) also undertook a review of studies that compared the lowest acceptable diagnostic mA for a range of chest CT examinations, including specific clinical indications such as GGO, pulmonary nodules, lymphoma, emboli and asbestos. The review looked at five CT studies conducted between 1998 and 2004, and the studies suggested that a current–time product of 20–50 mAs was sufficient for the detection of pulmonary nodules. In another part of Kubo's review, it was also noted that two other studies conducted between 2000 and 2003 reported decreased nodule detectability in images obtained with less than 20 mAs, as an exposure parameter; hence, this may be an important imaging threshold to evaluate [40]. Finally, when comparing LDCT with standard dose CT, there was no statistical significance in nodule detection (LDCT vs. Standard; 518 vs. 533), with varying nodule sizes: <3, 3–4.9, 5–6.9, 7–9.9 and ≥ 10 mm used in this and other studies [52–54].

Ground glass opacities and iterative reconstruction

Iterative reconstruction (IR) techniques has the ability to improve the image quality relative to the filtered back projection (FBP) techniques when undergoing low-dose chest CT [55]. The technical details of different proprietary IR techniques can be broad, but usually they are categorized into hybrid-based and model-based IR [56, 57]. Both their benefits and weakness are poorly understood and can lead to glossy images depending on which type of IR is employed [58]. In a recent study, it demonstrated that LDCT images demonstrated nonuniform noise in lung textured backgrounds and had somewhat degraded low-contrast spatial resolution [59]. In the current status, hybrid IR technique and LDCT imaging with 50 mAs enables noise and to maintain the detectability of GGO which is equivalent to the reference acquisitions of 200 mAs with filtered back projection [55]. While, at very low tube current at 10–20 mAs, the GGO attenuation is higher than the actual CT value with filtered back projection, with the potential of small GGO nodules could not be visualized because it was buried in increased noise that could be due to electronic noise because of the influence of the streak artifact. Equally, IR has been known to show that lower image noise, but did not provide any real improvement for radiologist's evaluation of thin-section (<2 mm) LDCT of the lung [60, 61]. Therefore, it is more important to employ the contrast to noise ratio with filtered back projection relative to the IR employed and the level of de-noising in order to maintain the actual CT value at use of use of low effective mAs [56, 57].

In summary, this article attempts to highlight some of the common chest CT signs that radiologists and emergency physicians are likely to encounter. With the increasing trend of using chest CT scans as an imaging tool to diagnose SARS-CoV-2, we emphasize that pattern recognition is the key, and this pictorial essay should serve as a guide to help establish a correct diagnosis coupled with correct scanner parameters to reduce radiation dose without affecting imaging quality in this tragic pandemic the world is facing.

Author contributions CS: guarantor of the study, CS and MR: study concepts and designs, CS: literature research, CS and MR: clinical studies, CS and MR: manuscript preparation, CS and MR: manuscript editing.

Funding No funding was needed for this article.

Compliance with ethical standards

Conflict of interest The authors declare that they have no conflict of interest.

Ethical approval This article does not contain any studies with human participants or animals performed by any of the authors.

Informed consent Informed consent was obtained from all individual participants included in the study.

References

1. Lai C-C et al. (2020) Severe acute respiratory syndrome coronavirus 2 (SARS-CoV-2) and corona virus disease-2019 (COVID-19): the epidemic and the challenges. Int J Antimicrobial Agents:105924
2. Porcheddu R et al (2020) Similarity in case fatality rates (CFR) of COVID-19/SARS-COV-2 in Italy and China. J Infect Dev Countries 14(02):125–128
3. Li Y, Xia L (2020) Coronavirus Disease 2019 (COVID-19): role of chest CT in diagnosis and management. Am J Roentgenol 214(6):1–7
4. Zu ZY et al (2020) Coronavirus Disease 2019 (COVID-19): a perspective from China. Radiology 296:200490
5. Chan M (2009) World now at the start of 2009 influenza pandemic
6. Chung M et al (2020) CT imaging features of 2019 novel coronavirus (2019-nCoV). Radiology 200230
7. Lei J et al. (2020) CT imaging of the 2019 novel coronavirus (2019-nCoV) pneumonia. Radiology 200236. https://doi.org/10.1148/radiol.2020200236
8. Bernheim A et al. (2020) Chest ct findings in coronavirus disease-19 (covid-19): relationship to duration of infection. Radiology 200463. https://doi.org/10.1148/radiol.2020200463
9. Pan F et al (2020) Time course of lung changes on chest CT during recovery from, novel coronavirus (COVID-19) pneumonia. Radiology 200370
10. Kanne JP (2019) Chest CT findings in, novel coronavirus (2019-nCoV) infections from Wuhan, China: key points for the radiologist. Radiology 200241. https://doi.org/10.1148/radiol.2020200241
11. Svahn TM, Sjöberg T, Ast JC (2019) Dose estimation of ultra-low-dose chest CT to different sized adult patients. Eur Radiol 29(8):4315–4323
12. Ludwig M et al (2019) Detection of pulmonary nodules: a clinical study protocol to compare ultra-low dose chest CT and standard low-dose CT using ASIR-V. BMJ Open 9(8):e025661
13. Sakane H et al. (2020) Biological effects of low-dose chest CT on chromosomal DNA. Radiology:190389
14. Liu K-C et al. (2020) CT manifestations of coronavirus disease-2019: a retrospective analysis of 73 cases by disease severity. Eur J Radiol 126:108941
15. Wang J et al. (2020) Dynamic changes of chest CT imaging in patients with corona virus disease-19 (COVID-19). Zhejiang da xue xue bao. Yi xue ban. J Zhejiang Univ Med Sci 49(1)
16. Protection R (2007) ICRP publication 103. Ann ICRP 37(2.4):2
17. Johns Hopkins Whiting School of Engineering website (2020) Coronavirus COVID-19 global cases. http://gisanddata.maps.arcgis.com/apps/opsdashboard/index.html#/bda7594740fd40299423467b48e9ecf6. Accessed 27 April 2020
18. Radiolgists RCO (2020) RCR position on the role of CT in patients suspected with COVID-19 infection. https://www.rcr.ac.uk/college/coronavirus-covid-19-what-rcr-doing/rcr-position-role-ct-patients-suspected-covid-19. Accessed 22 March 2020
19. Radiology ACO (2020) ACR recommendations for the use of chest radiography and computed tomography (CT) for suspected COVID-19 Infection. https://www.acr.org/Advocacy-and-Economics/ACR-Position-Statements/Recommendations-for-Chest-Radiography-and-CT-for-Suspected-COVID19-Infection. Accessed 22 March 2020
20. Mueller-Mang C, Ringl H, Herold C (2019) Interstitial lung diseases. In: Nikolaou K et al (eds) Multislice CT. Springer, Cham, pp 261–288
21. Webb WR (2006) Thin-section CT of the secondary pulmonary lobule: anatomy and the image—the 2004 Fleischner lecture. Radiology 239(2):322–338
22. Kandathil A, Chamarthy M (2018) Pulmonary vascular anatomy & anatomical variants. Cardiovasc Diagn Ther 8(3):201
23. Verschakelen JA, De Wever W (2018) Basic anatomy and CT of the normal lung. In: Computed tomography of the lung, Springer, p 3–19
24. Couture C (2017) Embryology, anatomy, and histology of the lung. In: Applied respiratory pathophysiology. CRC Press, p 1–14
25. Xu Z et al. (2020) Key points of clinical and CT imaging features of 2019 novel coronavirus (2019-nCoV) imported pneumonia based On 21 cases analysis. Available at SSRN 3543610
26. Pan Y et al (2020) Initial CT findings and temporal changes in patients with the novel coronavirus pneumonia (2019-nCoV): a study of 63 patients in Wuhan, China. Eur Radiol:1–4
27. Salehi S et al (2020) Coronavirus Disease 2019 (COVID-19): A Systematic Review of Imaging Findings in 919 Patients. Amer J Roentgenol 1–7
28. Martínez-Jiménez S, Rosado-de-Christenson ML, Carter BW (2017) Specialty Imaging: HRCT of the Lung E-Book. Elsevier, Amsterdam
29. Huang C et al (2020) Clinical features of patients infected with 2019 novel coronavirus in Wuhan, China. Lancet 395(10223):497–506
30. Bai HX et al (2020) Performance of radiologists in differentiating COVID-19 from viral pneumonia on chest CT. Radiology:200823
31. Gordic S et al (2014) Ultralow-dose chest computed tomography for pulmonary nodule detection
32. Kubo T et al (2014) Radiation dose reduction in chest CT—review of available options. Eur J Radiol 83(10):1953–1961
33. Costello JE et al (2013) CT radiation dose: current controversies and dose reduction strategies. Am J Roentgenol 201(6):1283–1290
34. Colletti PM, Micheli OA, Lee KH (2013) To shield or not to shield: application of bismuth breast shields. Am J Roentgenol 200(3):503–507
35. Wang J et al (2011) Radiation dose reduction to the breast in thoracic CT: comparison of bismuth shielding, organ-based tube current modulation, and use of a globally decreased tube current. Med Phys 38(11):6084–6092
36. Mussmann B et al. (2020) Organ-based tube current modulation in chest CT. A comparison of three vendors. Radiography
37. Hanley O et al (2017) Radiologists' recommendations for additional imaging on inpatient CT studies: Do referring physicians follow them? South Med J 110(12):770

38. Ishihara T et al. (2019) Impact of low-tube-voltage protocol on low-contrast detectability in ultra-high-resolution CT: an investigation for use of 1024 × 1024 and 2048 × 2048 matrix images. Eur Congr Radiol
39. van Ommen F et al (2019) Dose of CT protocols acquired in clinical routine using a dual-layer detector CT scanner: a preliminary report. Eur J Radiol 112:65–71
40. Kubo T et al (2008) Radiation dose reduction in chest CT: a review. Am J Roentgenol 190(2):335–343
41. Prakash P et al (2010) Is weight-based adjustment of automatic exposure control necessary for the reduction of chest ct radiation dose? Korean J Radiol 11(1):46–53
42. Christe A et al (2013) Accuracy of low-dose computed tomography (CT) for detecting and characterizing the most common CT-patterns of pulmonary disease. Eur J Radiol 82(3):e142–e150
43. Xie X et al (2014) Small irregular pulmonary nodules in low-dose CT: observer detection sensitivity and volumetry accuracy. Am J Roentgenol 202(3):W202–W209
44. Armato SG et al (2002) Lung cancer: performance of automated lung nodule detection applied to cancers missed in a CT screening program 1. Radiology 225(3):685–692
45. Båth M et al (2005) Nodule detection in digital chest radiography: introduction to the RADIUS chest trial. Radiat Prot Dosimetry 114(1–3):85–91
46. Prasad SR et al (2002) Standard-dose and 50%—reduced-dose chest CT: comparing the effect on image quality. Am J Roentgenol 179(2):461–465
47. Zhu X, Yu J, Huang Z (2004) Low-dose chest CT: optimizing radiation protection for patients. Am J Roentgenol 183(3):809–816
48. Li F et al (2002) Lung cancers missed at low-dose helical CT screening in a general population: comparison of clinical, histopathologic, and imaging findings 1. Radiology 225(3):673–683
49. Christe A et al (2013) Impact of image quality, radiologists, lung segments, and Gunnar eyewear on detectability of lung nodules in chest CT. Acta Radiol 54(6):646–651
50. Cheng Y et al (2019) Validation of algorithmic CT image quality metrics with preferences of radiologists. Med Phys 46(11):4837–4846
51. Mettler FA Jr et al (2008) Effective doses in radiology and diagnostic nuclear medicine: a catalog 1. Radiology 248(1):254–263
52. Karabulut N et al (2002) Comparison of low-dose and standard-dose helical CT in the evaluation of pulmonary nodules. Eur Radiol 12(11):2764–2769
53. Mazzei FG et al. (2014) Reduced time CT perfusion acquisitions are sufficient to measure the permeability surface area product with a deconvolution method. BioMed Res Int 2014
54. Mazzei MA et al (2013) La perfusione con TC nella caratterizzazione del nodulo polmonare solitario: possibilità e limiti in uno studio preliminare. Recenti Prog Med 104(7):430–437
55. Higuchi K et al (2013) Detection of ground-glass opacities by use of hybrid iterative reconstruction (iDose) and low-dose 256-section computed tomography: a phantom study. Radiol Phys Technol 6(2):299–304
56. Pontana F et al (2011) Chest computed tomography using iterative reconstruction vs filtered back projection (Part 2): image quality of low-dose CT examinations in 80 patients. Eur Radiol 21(3):636–643
57. Pontana F et al (2011) Chest computed tomography using iterative reconstruction vs filtered back projection (Part 1): evaluation of image noise reduction in 32 patients. Eur Radiol 21(3):627–635
58. Willemink MJ et al (2013) Iterative reconstruction techniques for computed tomography Part 1: technical principles. Eur Radiol 23(6):1623–1631
59. Solomon J et al. (2020) Noise and spatial resolution properties of a commercially available deep-learning based CT reconstruction algorithm. Med Phys
60. Pavarani A et al (2016) Effect of iterative reconstruction on image quality of low-dose chest computed tomography. Acta Biomed 87(2):168–176
61. Lim H-J et al (2016) The impact of iterative reconstruction in low-dose computed tomography on the evaluation of diffuse interstitial lung disease. Korean J Radiol 17(6):950–960

Publisher's Note Springer Nature remains neutral with regard to jurisdictional claims in published maps and institutional affiliations.